A multi-scale approach to model the curing process in magneto-sensitive polymeric materials

Mokarram Hossain [a], George Chatzigeorgiou [b], Fodil Meraghni [b], Paul Steinmann [a,*]

[a] Chair of Applied Mechanics, University of Erlangen-Nuremberg, Egerlandstr. 5, 91058 Erlangen, Germany
[b] LEM3-UMR 7239 CNRS, Arts et Métiers ParisTech Metz-Lorraine, 4 Rue Augustin Fresnel 57078 Metz, France

A B S T R A C T

We propose a magneto-mechanically coupled multi-scale model for simulating the curing process of polymers. In the case of magneto-sensitive polymers, micron-size ferromagnetic particles are mixed with a liquid polymeric matrix in the uncured stage. The polymer curing process is a complex process that transforms a fluid to a solid with time. To transfer the constituent parameter information from the micro-scale to the macro-scale for a composite magneto-mechanically coupled polymeric material, an extended Mori–Tanaka semi-analytic homogenization procedure is utilized. The stiffness gaining phenomenon as in the case of a curing process is realized by time-dependent material parameters appearing within the composite piezomagnetic material tensors. Moreover, to compute the volume reduction during curing, a magnetic induction dependent shrinkage model is proposed. Several numerical examples show that the model proposed herein can capture major observable phenomena in the curing process of polymers under magneto-mechanically coupled infinitesimal deformations.

1. Introduction and outline

Recently magnetorheological elastomers (MREs) became a new class of smart materials. The basic mechanism in MREs is that under an external magnetic excitation, their mechanical properties can be altered. They are relatively a new group in the realm of so-called smart materials. Due to the magnetically controllable stiffness and damping behavior, they are attractive candidates for various technical applications, e.g. suspension bushing, brakes, clutches, smart springs in dynamic vibration absorber to civil engineering devices such as building vibration isolators (Boczkowska and Awietjan, 2009; Böse et al., 2012; Jolly et al., 1996; Varga et al., 2006; Danas et al., 2012; Kaleta et al., 2011; Zhou, 2003; Chen et al., 2007).

In the curing process of polymers, a viscoelastic fluid transforms into a viscoelastic solid due to a series of chemical reactions. Such reactions result in polymer chains cross-linking to each other and formation of chemical bonds allow the chains to come closer. The packing of chains due to cross-linking will yield a decrease in specific volume which is denoted as the volume or curing shrinkage. For an illustrative review on the constitutive modeling of the curing process of polymers, our previous works, cf. Hossain et al. (2009a,b) can be considered. In developing a cure-dependent small strain constitutive model for a thermosetting polymer, Kiasat (2000) assumed that the formation of new cross-links during curing does not affect the current stress state caused by previously applied strains, i.e. new cross-links form unstrained and stress-free. Several researches agree with this assumption (Hojjati et al., 2004; Gillen, 1988). Lion and co-workers (Liebl et al., 2012; Lion and Höfer, 2007; Johlitz, 2012; Johlitz and Lion, 2013) proposed a phenomenologically-inspired viscoelastic curing model. In order to model the evolution of material parameters during curing, they introduce the so-called intrinsic time concept which is then related to the degree of cure, a key parameter to quantify the state and the completeness of a curing process. For more models on the curing process, see Mahnken (2013) and Heinrich et al. (2013) et al.

It is well established nowadays that composite material's overall behavior depends strongly on the properties of the material constituents and the microscopic geometry, i.e. the volume fraction, shape and orientation of constituents. Homogenization methods, as pioneered by Hill (1963) and Hill and Rice (1972), allow to study the overall mechanical behavior of composites with general and periodic microstructures (Hashin and Shtrikman, 1963; Bensoussan et al., 1978; Mura, 1987; Murat and Tartar, 1995;

Kouznetsova et al., 2001; Miehe and Koch, 2002). Homogenization of composites with linear as well as nonlinear constituents has been studied extensively (Suquet, 1987; Guedes and Kikuchi, 1990; Terada and Kikuchi, 1995; Aboudi et al., 2003; Ponte Castañeda, 1996; Smit et al., 1998; Feyel and Chaboche, 2000; Michel et al., 1999; Terada and Kikuchi, 2001; Asada and Ohno, 2007; Miehe, 2002; Yvonnet J et al., 2009) and thorough reviews of different multi-scale approaches are available in the literature (Pindera et al., 2009; Kanouté et al., 2009; Charalambakis, 2010; Geers et al., 2010). Such averaging approaches have also been considered for the magneto-mechanical response of magnetorheological elastomers (Borcea and Bruno, 2001; Yin et al., 2002; Wang et al., 2003; Yin et al., 2006; Ponte Castañeda and Galipeau, 2011; Galipeau and Ponte Castañeda, 2013; Javili et al., 2014; Chatzigeorgiou et al., 2014). In this paper, a modified version of the Mori–Tanaka method is utilized. The differences between the classical mean-field theories (Eshelby dilute approach, Mori–Tanaka and self-consistent) have been extensively discussed in several books (Qu and Cherkaoui, 2006; Mura, 1987). These three averaging homogenization techniques are based on the Eshelby's equivalent inclusion theory (Mura, 1987). In brief: it is commonly established that the Eshelby dilute approach provides reliable estimations only for small particles volume fractions, whereas Mori–Tanaka and self-consistent are acceptable also for moderate particle volume fractions. However, self-consistent is an iterative method even in elasticity, and it is generally and extensively used to describe polycrystalline material structures. Mori–Tanaka does not require iterations in the elasticity problem and is more efficient in the case of matrix-particle type of composites, where the particles can have arbitrary orientation.

Several experimental works demonstrate the formation of isotropic and anisotropic magneto-sensitive polymeric composites during the curing process with or without the application of a magnetic induction (Jolly et al., 1996; Varga et al., 2006; Danas et al., 2012; Kaleta et al., 2011; Zhou, 2003; Chen et al., 2007). However, there is a lack of constitutive modeling that can capture the curing process in the presence of a magneto-mechanically coupled load. Several multi-scale approaches are developed for magneto-sensitive polymers with coupled loads where the constitutive material parameters appearing in a model are non-evolving (Schröder and Keip, 2012; Javili et al., 2014). Moreover, a multi-scale approach is proposed during the curing process in which parameters are considered to be evolving with time (Klinge et al., 2012,). However, in the latter works, only a mechanical load is considered during the curing process. To the authors best knowledge, there is currently no multi-scale approach that can capture homogenized behavior as well as can predict the stiffness gaining process in the presence of a magneto-mechanically coupled load. The simulation of microheterogeneous polymers, especially particle-filled magneto-sensitive composites during the curing process, can be studied using various homogenization techniques. The numerical homogenization approach is especially suitable for the simulation of heterogeneous materials with a highly oscillatory microstructure, cf. Klinge et al. (2012,).

The main framework of the proposed model is within the hypoelastic concept of our previously proposed purely mechanical curing model (Hossain et al., 2009a) which is recently extended to the case of particle-filled magneto-sensitive polymers at finite strains (Hossain et al., 2015a). The earlier works that appeared in Hossain et al. (2009a, 2014), on the one hand, are only for phenomenologically-motivated curing modeling under a purely mechanical load. This is for the case of unfilled polymers. On the other hand, the recent works published in Hossain et al. (2015a,b) consider the magneto-mechanically coupled load. Thereby, the main contribution of Hossain et al. (2015a,b) is a phenomenologically-motivated modeling framework for the curing modeling for magnetizable particle-filled polymers. The constitutive model proposed in the current manuscript transfers the constituent parameter information from the micro-scale to the macro-scale for a magneto-mechanically coupled composite at each time step of the curing evolution. The effective parameters of magnetic particle-filled polymers are coming from composite micromechanics rather than taking a continuum parameter set as in the previous two contributions. As a first step in the multi-scale modeling during the curing process, we herein propose a micromechanical approach for small magneto-mechanically coupled deformations where a time-dependence of the mechanical parameters appearing in the constitutive relation is considered. The curing phenomenon is a highly temperature-sensitive and exothermic reaction process. However, for simplicity, we develop the cure-dependent magneto-mechanical coupled model for the case of isothermal processes.

Section 2 discusses the main mathematical foundation that leads to a hypoelastic type constitutive relation for the polymer curing process in the presence of a magneto-mechanically coupled load. In Section 3, a magnetic load dependent curing shrinkage model is proposed where the duration and magnitude of the load is taken into account while the evolution of relevant material parameters is expressed in Section 4. The main mathematical framework to transfer the micro-scale information to the macro-scale is described in Section 5 while the corresponding numerical discretization procedures are elaborated in Section 6. Several numerical examples by pure mechanical, pure magnetic as well as magneto-mechanically coupled loads are presented in Section 7 along with a few illustrative examples for the shrinkage-induced stress generation for a magnetic load dependent curing process.

2. Modeling curing in nonlinear magneto-elasticity

In polymer curing processes, successive chemical reactions yield a cross-linked structure from an initial solution of monomers. This phase transition is analogous to the addition of more and more springs to the already-formed network. According to the literature (Kiasat, 2000; Gillen, 1988), the formation of a new cross-link is unstrained and stress-free. It means that a curing material does not change its state of stress as resulted from previous deformations – even though its material properties continue to evolve. Keeping the above mentioned physical fact in mind, a magneto-elastic coupled energy potential for the case of isothermal curing processes is proposed in the form of a convolution integral as

$$\begin{aligned}\Phi(\boldsymbol{\varepsilon},\mathbb{b},t) = \frac{1}{2}\int_0^t \big[\boldsymbol{\mathcal{A}}'(\tau) : [\boldsymbol{\varepsilon}(t)-\boldsymbol{\varepsilon}(\tau)]\big] \\ : [\boldsymbol{\varepsilon}(t)-\boldsymbol{\varepsilon}(\tau)]d\tau + \frac{1}{2}\int_0^t [\boldsymbol{\mathcal{K}}'(\tau)\cdot[\mathbb{b}(t)-\mathbb{b}(\tau)]] \\ \cdot [\mathbb{b}(t)-\mathbb{b}(\tau)]d\tau + \int_0^t [\boldsymbol{\mathcal{C}}'(\tau)\cdot[\mathbb{b}(t)-\mathbb{b}(\tau)]] \\ : [\boldsymbol{\varepsilon}(t)-\boldsymbol{\varepsilon}(\tau)]d\tau \end{aligned} \tag{1}$$

where $\boldsymbol{\mathcal{A}}'(\tau) = d\boldsymbol{\mathcal{A}}(\tau)/d\tau$, $\boldsymbol{\mathcal{K}}'(\tau) = d\boldsymbol{\mathcal{K}}(\tau)/d\tau$ and $\boldsymbol{\mathcal{C}}'(\tau) = d\boldsymbol{\mathcal{C}}(\tau)/d\tau$. In Eq. (1) $\boldsymbol{\varepsilon}$ is the infinitesimal strain, $\mathbb{b}$ is the magnetic induction vector and t is the curing time. A finite strain version of the potential function proposed in Eq. (1) and its corresponding derivations are given in Hossain et al. (2015a). Note that $\boldsymbol{\mathcal{A}}$ is the fourth order mechanical stiffness tensor, $\boldsymbol{\mathcal{K}}$ is the second order magnetic permeability tensor, and $\boldsymbol{\mathcal{C}}$ is the third order coupled magnetomechanical tensor, where the material parameters appearing within the tensors are generally time-dependent. Specific forms of these tensors are given in Section 7. The second law of thermodynamics in the form

of the Clausius–Duhem inequality for an isothermal process can be written in the case of a magneto-elastic problem as

$$\boldsymbol{\sigma} : \dot{\boldsymbol{\varepsilon}} + \mathbb{h} \cdot \dot{\mathbb{b}} - \dot{\Phi} \geqslant 0, \tag{2}$$

where $\boldsymbol{\sigma}$, $\mathbb{h}$ and Φ are the stress tensor, the magnetic field vector and the potential function from Eq. (1), respectively. In Eq. (2), $(\dot{\bullet})$ is a time derivative. To evaluate the above dissipation inequality, the time derivative of the energy potential Φ follows from adopting the Leibniz integral rule. The standard Coleman–Noll procedure provides the following functional for the stress $\boldsymbol{\sigma}$ and the magnetic field $\mathbb{h}$:

$$\begin{aligned}
\boldsymbol{\sigma}(\boldsymbol{\varepsilon}, \mathbb{b}, t) &= \int_0^t \boldsymbol{\mathcal{A}}'(\tau) : [\boldsymbol{\varepsilon}(t) - \boldsymbol{\varepsilon}(\tau)] d\tau + \int_0^t \boldsymbol{\mathcal{C}}'(\tau) \cdot [\mathbb{b}(t) - \mathbb{b}(\tau)] d\tau, \\
\mathbb{h}(\boldsymbol{\varepsilon}, \mathbb{b}, t) &= \int_0^t \boldsymbol{\mathcal{C}}^{t'}(\tau) : [\boldsymbol{\varepsilon}(t) - \boldsymbol{\varepsilon}(\tau)] d\tau + \int_0^t [\boldsymbol{\mathcal{K}}'(\tau) \cdot [\mathbb{b}(t) - \mathbb{b}(\tau)]] d\tau.
\end{aligned} \tag{3}$$

In deriving the above expressions, permutability of the double and single contractions are required which are given since $\boldsymbol{\mathcal{A}}$ and $\boldsymbol{\mathcal{K}}$ possess symmetries, cf. Hossain et al. (2015a). To obtain more precise relations among stress, strain, magnetic field and magnetic induction, the Leibniz integral rule has to be applied once more to yield

$$\begin{aligned}
\dot{\boldsymbol{\sigma}}(\boldsymbol{\varepsilon}, \mathbb{b}, t) &= \boldsymbol{\mathcal{A}}(t) : \dot{\boldsymbol{\varepsilon}}(t) + \boldsymbol{\mathcal{C}}(t) \cdot \dot{\mathbb{b}}(t), \\
\dot{\mathbb{h}}(\boldsymbol{\varepsilon}, \mathbb{b}, t) &= \boldsymbol{\mathcal{C}}^t(t) : \dot{\boldsymbol{\varepsilon}}(t) + \boldsymbol{\mathcal{K}}(t) \cdot \dot{\mathbb{b}}(t).
\end{aligned} \tag{4}$$

In micromechanics it is more convenient to write the last expressions in terms of the rates of strain and magnetic field instead of strain and magnetic induction (Chatzigeorgiou et al., 2014). Thus, rearranging them and accounting for the symmetry of $\boldsymbol{\mathcal{K}}$ yields

$$\begin{aligned}
\dot{\boldsymbol{\sigma}}(\boldsymbol{\varepsilon}, \mathbb{h}, t) &= \boldsymbol{\mathcal{A}}_{\mathbb{h}}(t) : \dot{\boldsymbol{\varepsilon}}(t) + \boldsymbol{\mathcal{C}}_{\mathbb{h}}(t) \cdot [-\dot{\mathbb{h}}(t)], \\
\dot{\mathbb{b}}(\boldsymbol{\varepsilon}, \mathbb{h}, t) &= \boldsymbol{\mathcal{C}}^t_{\mathbb{h}}(t) : \dot{\boldsymbol{\varepsilon}}(t) - \boldsymbol{\mathcal{K}}_{\mathbb{h}}(t) \cdot [-\dot{\mathbb{h}}(t)],
\end{aligned} \tag{5}$$

where

$$\begin{aligned}
\boldsymbol{\mathcal{A}}_{\mathbb{h}}(t) &= \boldsymbol{\mathcal{A}}(t) + \boldsymbol{\mathcal{C}}_{\mathbb{h}}(t) \cdot \boldsymbol{\mathcal{C}}^t(t), \\
\boldsymbol{\mathcal{C}}_{\mathbb{h}}(t) &= -\boldsymbol{\mathcal{C}}(t) \cdot \boldsymbol{\mathcal{K}}^{-1}(t), \quad \boldsymbol{\mathcal{K}}_{\mathbb{h}}(t) = \boldsymbol{\mathcal{K}}^{-1}(t).
\end{aligned} \tag{6}$$

Note that in general for nonlinear magnetoelastic continua, the magnetomechanical moduli $\boldsymbol{\mathcal{A}}_{\mathbb{h}}$, $\boldsymbol{\mathcal{C}}_{\mathbb{h}}$ and $\boldsymbol{\mathcal{K}}_{\mathbb{h}}$ have a complicated dependence on time as well as on the current loading status, i.e.

$$\begin{aligned}
&\boldsymbol{\mathcal{A}}_{\mathbb{h}}(t) \equiv \boldsymbol{\mathcal{A}}_{\mathbb{h}}(\boldsymbol{\varepsilon}(t), \mathbb{h}(t), t), \quad \boldsymbol{\mathcal{C}}_{\mathbb{h}}(t) \equiv \boldsymbol{\mathcal{C}}_{\mathbb{h}}(\boldsymbol{\varepsilon}(t), \mathbb{h}(t), t), \\
&\boldsymbol{\mathcal{K}}_{\mathbb{h}}(t) \equiv \boldsymbol{\mathcal{K}}_{\mathbb{h}}(\boldsymbol{\varepsilon}(t), \mathbb{h}(t), t).
\end{aligned} \tag{7}$$

3. Shrinkage modeling

In the case of modeling curing-induced shrinkage, an additive decomposition of the total strain into a mechanical part and a shrinkage-induced part is proposed in our previous purely mechanical curing modeling approach for an isotropic unfilled polymer, cf. Hossain et al. (2009a), i.e.

$$\boldsymbol{\varepsilon} = \boldsymbol{\varepsilon}_m + \boldsymbol{\varepsilon}_s = \boldsymbol{\varepsilon}_m + s(t)\boldsymbol{I}, \quad [I]_{ij} = \delta_{ij} \tag{8}$$

where

$$s(t) = s_\infty [1 - \exp(-\beta_s t)] \tag{9}$$

and s_∞, β_s is the total volume shrinkage and a curvature parameter, respectively. Note that Eq. (9) is one of the simplest forms of exponential saturation functions to assess the evolution of the curing-induced volume reduction. Other forms of expressions can be incorporated easily. The curing shrinkage can be included, following the arguments in the case of a purely mechanical loading, cf. Hossain et al. (2009a), to the constitutive relation as

$$\dot{\boldsymbol{\sigma}}(\boldsymbol{\varepsilon}, \mathbb{b}, t) = \boldsymbol{\mathcal{A}} : [\dot{\boldsymbol{\varepsilon}}(t) - \dot{\boldsymbol{\varepsilon}}_s(t)] + \boldsymbol{\mathcal{C}} \cdot \dot{\mathbb{b}}(t). \tag{10}$$

This implies that in the absence of any external loading, either a mechanical or a magnetic or both, there will be an internal strain due to the packing of polymer molecules during a curing process which will generate stresses if a sample is held fixed. Under the influence of a magneto-mechanical load, in contrast to the curing process under a pure mechanical load as formulated in Hossain et al. (2009a), we assume here that there is a coupled relation between the total amount of curing shrinkage and the applied magnetic induction, i.e.

$$s(t, \mathbb{b}) = s_\infty(t, \mathbb{b})[1 - \exp(-\beta_s t)]. \tag{11}$$

Now, we define a new parameter 'degree of exposure' e that accounts for the overall influence of a magnetic load on the curing process. It is formulated as

$$e = \int_0^t f(\alpha(\tau)) |\mathbb{b}(\tau)| d\tau, \quad \text{with,} \quad f(\alpha) = 1 - H(\alpha - 1), \tag{12}$$

where H is the Heaviside function and $|\mathbb{b}(\tau)|$ is the magnitude of the applied magnetic induction. The parameter e determines how long a curing sample is exposed to the applied magnetic load. The function $f(\alpha)$ inculcates the fluctuating influence of a magnetic load to the model, i.e. if the sample is fully cured, it has no impact in the degree of exposure. Two extreme values of exposure are defined as $0 < e_1 < e_2$. These simply imply that when the lower value of the degree of exposure e crosses the threshold e_1 it starts increasing the value of the shrinkage parameter s from an initial value of s_1. When it reaches the upper threshold value e_2, the maximum possible value of shrinkage $s = s_2$ is reached and the evolution of s remains unchanged. All these information can be incorporated once the evolution of s can be expressed by the following functional form

$$s_\infty(t, \mathbb{b}) = \frac{s_1 + s_2}{2} + \frac{s_2 - s_1}{2} \tanh\left(\xi \left[e - \frac{1}{2}[e_1 + e_2]\right]\right), \tag{13}$$

where ξ is a scaling constant.

4. Time-dependent parameters during curing

One physically sound assumption in the case of polymer curing is considered in developing the constitutive model, i.e. all relevant material parameters in a model will be time-dependent. Some parameters are related to pure mechanical phenomena while others are for coupled processes. Following the analogy of the purely mechanical curing, we make reasonable choices for modeling the temporal evolution of the material parameters due to the present lack of sufficient experimental data. One of the easiest formats for the evolving parameters can be an exponential saturation function as

$$q(t) = q_0 + [q_\infty - q_0]\left[1 - \exp(-\kappa_q t)\right], \tag{14}$$

which is being governed by the initial and the final values q_0 and q_∞, respectively, as well as the curvature parameter κ_q. In the case of the shear modulus evolution, the initial and final cut-off values, i.e. q_0 and q_∞, respectively, are replaced by μ_0 and μ_∞, while the curvature parameter κ_q is substituted by κ_μ. According to several papers (Chen et al., 2007; Xu et al., 2011), the coupled magneto-mechanical parameters also evolve following the format of an exponential saturation function. The exponential form for the evolution of the curing parameter $q(t)$ (similar to the degree of cure) is one of the simplest forms that can take into account the time-dependence of the process. It replicates the most commonly obtained shape, i.e. exponentially increasing saturation function, of the curing kinetics of any polymer vastly documented in the literature (Lion and Höfer, 2007; Kiasat, 2000; Hojjati et al., 2004). As it will be shown later by the multi-scale analysis, such a behavior

appears in the composite magnetomechanical materials even if the matrix (here an epoxy) is magnetically inactive.

5. Multi-scale approach in curing magneto-elasticity

5.1. Without shrinkage effects

When considering a composite material, Eq. (5) apply to each constituent whose material properties are known. The identification of the composite properties and response can be achieved through micromechanics methodologies. Here the Mori–Tanaka approach is employed, extended to magnetomechanical materials. The main theory has been developed in Dunn and Taya (1993) and in this section a brief description of the extended Mori–Tanaka approach is provided.

Using indicial notation along with Einstein summation convention, Eq. (5) can be represented in a more general way,

$$\dot{\Sigma}_{ij} = \mathcal{L}_{ijmn}(\boldsymbol{E},t)\dot{E}_{mn}, \tag{15}$$

with

$$\Sigma_{ij} = \begin{cases} \sigma_{ij}, & i=1,2,3, \\ b_j, & i=4, \end{cases} \quad E_{mn} = \begin{cases} \varepsilon_{mn}, & m=1,2,3, \\ -\mathbb{h}_n, & m=4, \end{cases}$$
$$\mathcal{L}_{ijmn}(\boldsymbol{E},t) = \begin{cases} \mathcal{A}_{\mathbb{h}_{ijmn}}(\boldsymbol{E},t), & i,\ m=1,2,3, \\ \mathcal{C}_{\mathbb{h}_{nij}}(\boldsymbol{E},t), & i=1,2,3,\ m=4, \\ \mathcal{C}_{\mathbb{h}_{jmn}}(\boldsymbol{E},t), & i=4,\ m=1,2,3, \\ -\mathcal{K}_{\mathbb{h}_{jn}}(\boldsymbol{E},t), & i,\ m=4. \end{cases} \tag{16}$$

Assuming a composite of $N+1$ phases, the magnetomechanical properties of both the polymeric matrix (index 0) and the different types of particles (index 1 to N) are considered to obey a constitutive law of the above form (15). For nonlinear magnetoelastic continua, $\mathcal{L}$ is a known function of $\boldsymbol{E}$ and time. The scope of micromechanics is to identify the overall properties of the composite that satisfy a similar constitutive law, i.e.

$$\dot{\bar{\boldsymbol{\Sigma}}} = \bar{\mathcal{L}} : \dot{\bar{\boldsymbol{E}}}, \tag{17}$$

where the bar above a symbol indicates macroscopic variable or property. According to the usual assumptions in micromechanics, the particles are considered randomly dispersed inside the matrix and the overall tensors $\bar{\boldsymbol{\Sigma}}$ and $\bar{\boldsymbol{E}}$ are equal to the volume integrals of the respective tensors $\boldsymbol{\Sigma}_r$ and $\boldsymbol{E}_r$ of the material constituents ($r=0,\ldots,N$),

$$\bar{\boldsymbol{\Sigma}} = \sum_{r=0}^{N} c_r \boldsymbol{\Sigma}_r, \quad \bar{\boldsymbol{E}} = \sum_{r=0}^{N} c_r \boldsymbol{E}_r, \tag{18}$$

with c_r being the volume fraction of the r_{th} phase (0 for the matrix and $1,\ldots,N$ for the particles). Although, for this particular problem at hand we consider only one type of filler particle, we keep N for the sake of generality of the proposed modeling framework.

Eq. (15) provides a time dependent magnetomechanical (rate form) type constitutive law. Since $\mathcal{L}$ in nonlinear magnetoelastic continua depends on $\boldsymbol{E}$, the direct connection between the tensors $\boldsymbol{\Sigma}_r$ and $\boldsymbol{E}_r$ is very difficult, if possible, to be obtained. In order to be able to proceed, one can assume that the relations (15) hold in the same spirit for average quantities, i.e.

$$\dot{\bar{\boldsymbol{\Sigma}}}_r = \mathcal{L}_r(\boldsymbol{E}_r,t) : \dot{\boldsymbol{E}}_r. \tag{19}$$

Such a simplification has been shown to work quite well in the case of elastoplastic composites (Lagoudas et al., 1991).

Using the extended version (19) for the material constitutive laws, the generalized Mori–Tanaka strain concentration tensors of the constituents are given by[1] (Dunn and Taya, 1993; Qu and Cherkaoui, 2006)

$$\boldsymbol{T}_r^{\text{MT}} = \boldsymbol{T}_r^{\text{dil}} : \left[\sum_{r=0}^{N} c_r \boldsymbol{T}_r^{\text{dil}}\right]^{-1}. \tag{20}$$

In the above expression $\boldsymbol{T}_r^{\text{dil}}$ is the dilute strain concentration tensor of each phase, computed by the relation

$$\boldsymbol{T}_r^{\text{dil}} = \left[\mathcal{I} + \mathcal{S}_r : \mathcal{L}_0^{-1} : [\mathcal{L}_r - \mathcal{L}_0]\right]^{-1}, \tag{21}$$

where $\mathcal{I}$ is the fourth order symmetric identity tensor. Obviously, for the matrix it holds $\boldsymbol{T}_0^{\text{dil}} = \mathcal{I}$. The Eshelby tensors $\mathcal{S}_r$ of the particles are provided by the fundamental solution of the Eshelby problem and depend on the shapes of the particles as well as the polymeric matrix properties (Dunn and Taya, 1993). For general ellipsoidal shapes of the particles and non-isotropic matrix, the Eshelby tensor can be obtained numerically through the procedure described in Gavazzi and Lagoudas (1990), extended to the case of magnetomechanical materials. The Eshelby tensor for an ellipsoidal inclusion with main axes $a_1,\ a_2,\ a_3$ (Fig. 1) is given in indicial notation by the formula

$$\mathcal{S}_{ijkl} = \begin{cases} \frac{1}{8\pi}\mathcal{L}_{0_{mnkl}} \int_{-1}^{1} \int_{0}^{2\pi} \left[\hat{\zeta}_j\hat{\zeta}_n\mathcal{Z}_{im}^{-1} + \hat{\zeta}_i\hat{\zeta}_n\mathcal{Z}_{jm}^{-1}\right] d\omega d\zeta_3, & i=1,2,3, \\ \frac{1}{4\pi}\mathcal{L}_{0_{mnkl}} \int_{-1}^{1} \int_{0}^{2\pi} \hat{\zeta}_j\hat{\zeta}_n\mathcal{Z}_{4m}^{-1} d\omega d\zeta_3, & i=4, \end{cases} \tag{22}$$

with

$$\hat{\zeta}_1 = \sqrt{1-\zeta_3}\frac{\cos\omega}{a_1}, \quad \hat{\zeta}_2 = \sqrt{1-\zeta_3}\frac{\sin\omega}{a_2}, \quad \hat{\zeta}_3 = \frac{\zeta_3}{a_3}, \quad \mathcal{Z}_{ik} = \mathcal{L}_{0_{ijkl}}\hat{\zeta}_j\hat{\zeta}_l. \tag{23}$$

Eq. (22) can be solved numerically using a Gaussian quadrature formula (Gavazzi and Lagoudas, 1990).

With the help of the generalized Mori–Tanaka strain concentration tensor (20) the effective magnetomechanical tangent modulus is computed by the equation

$$\bar{\mathcal{L}} = \sum_{r=0}^{N} c_r \mathcal{L}_r : \boldsymbol{T}_r^{\text{MT}}. \tag{24}$$

As a remark, the dilute and Mori–Tanaka stress concentration tensors of each phase are given by

$$\boldsymbol{H}_r^{\text{dil}} = \mathcal{L}_r : \boldsymbol{T}_r^{\text{dil}} : \mathcal{L}_0^{-1} \tag{25}$$

and

$$\boldsymbol{H}_r^{\text{MT}} = \boldsymbol{H}_r^{\text{dil}} : \left[\sum_{r=0}^{N} c_r \boldsymbol{H}_r^{\text{dil}}\right]^{-1}, \tag{26}$$

respectively. For purely linear, transversely isotropic, magnetoelastic materials with one type of spherical particles, lengthy analytical expressions can be obtained (see Levin et al. (2000)).

5.2. With shrinkage effects

The shrinkage of the polymeric matrix during curing introduces additional strains, as indicated by Eq. (8). These internally generated strains are mainly dependent on time as the curing process proceeds. Their dependence on the magnetic induction practically appears only in a short range of $\mathbb{h}$, as Eqs. (11) and (13) indicate. One way to account for these additional strains in the Mori–Tanaka scheme is to treat them as an inhomogeneous inhomogeneity (Qu and Cherkaoui, 2006), i.e. the material constituents of the composite possess their own strains.

The constitutive relations in the case of curing with shrinkage can be written in a general form as

[1] The inverse of a fourth order tensor $\mathcal{B}$ with minor symmetries is defined as the fourth order tensor $\mathcal{B}^{-1}$ whose components are identified from the relation $\mathcal{B}_{ijkl}\mathcal{B}^{-1}_{klmn} = \mathcal{I}_{ijmn} = \frac{1}{2}[\delta_{im}\delta_{jn} + \delta_{in}\delta_{jm}]$ with δ_{ij} being the Kronecker delta.

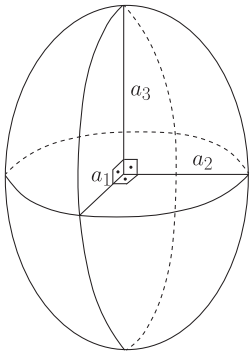

Fig. 1. Ellipsoidal inclusion.

$$\dot{\Sigma}_{ij} = \mathcal{L}_{ijmn}\left[\dot{E}_{mn} - \dot{E}_{s_{mn}}\right], \tag{27}$$

with the generalized shrinkage tensor $\boldsymbol{E}_s$ given by

$$E_{s_{mn}} = \begin{cases} \varepsilon_{s_{mn}}, & m = 1,2,3, \\ 0, & m = 4, \end{cases} \tag{28}$$

where $\varepsilon_{s_{mn}} = s(t)\boldsymbol{I}_{mn}$and $s(t)$ is given by Eq. (9). The rest of the tensors are given by (16).

Following the same approach as Lester et al. (2011), extended to magnetomechanical materials, the macroscopic generalized shrinkage tensor is provided by the relation

$$\bar{\boldsymbol{E}}_s = \sum_{r=0}^{N} c_r \boldsymbol{E}_{s,r} + \sum_{r=1}^{N} c_r \left[\mathcal{I} - \bar{\mathcal{L}}^{-1} : \mathcal{L}_r\right] : \mathcal{R}_r : [\boldsymbol{E}_{s,r} - \boldsymbol{E}_{s,0}], \tag{29}$$

where $\boldsymbol{E}_{s,r}$ is the generalized shrinkage tensor for each material ($r = 0$ for the matrix and $r = 1,\ldots,N$ for the particles), $\bar{\mathcal{L}}$ is given by Eq. (24) and

$$\mathcal{R}_r = \mathcal{S}_r : [[\mathcal{L}_r - \mathcal{L}_0] : \mathcal{S}_r + \mathcal{L}_0]^{-1} : \mathcal{L}_r - \mathcal{I}. \tag{30}$$

Obviously, the metallic particles do not undergo curing and shrinkage, thus $\boldsymbol{E}_{s,r} = \boldsymbol{0}$ for $r \neq 0$. Eq. (29) indicates that the composite generalized shrinkage strain tensor is not necessarily isotropic, even if the matrix displays an isotropic response (Eq. (8)). The final shrinkage behavior of the composite depends also on the particles material properties, their shape and the way they are distributed inside the matrix.

For a given macroscopic strain-type tensor $\bar{\boldsymbol{E}}$, the stress-type macroscopic tensor $\bar{\boldsymbol{\Sigma}}$ is computed from the macroscopic constitutive law

$$\dot{\bar{\boldsymbol{\Sigma}}} = \bar{\mathcal{L}} : [\dot{\bar{\boldsymbol{E}}} - \dot{\bar{\boldsymbol{E}}}_s]. \tag{31}$$

With this information one can compute the stress-type tensors for each material constituent through the formulas

$$\boldsymbol{\Sigma}_r = \boldsymbol{H}_r^{\mathrm{MT}} : \left[\bar{\boldsymbol{\Sigma}} - \sum_{n=1}^{N} c_n \mathcal{L}_n : \mathcal{R}_n : [\boldsymbol{E}_{s,n} - \boldsymbol{E}_{s,0}]\right] + \mathcal{L}_r : \mathcal{R}_r : [\boldsymbol{E}_{s,r} - \boldsymbol{E}_{s,0}], \tag{32}$$

for $r = 1,\ldots,N$ and

$$\boldsymbol{\Sigma}_0 = \boldsymbol{H}_0^{\mathrm{MT}} : \left[\bar{\boldsymbol{\Sigma}} - \sum_{n=1}^{N} c_n \mathcal{L}_n : \mathcal{R}_n : [\boldsymbol{E}_{s,n} - \boldsymbol{E}_{s,0}]\right], \tag{33}$$

where the $\boldsymbol{H}_r^{\mathrm{MT}}$ is given by Eq. (26). The strain-type tensors for each constituent thus can be computed from the materials constitutive laws, i.e.

$$\dot{\boldsymbol{E}}_r = \mathcal{L}_r^{-1} : \dot{\boldsymbol{\Sigma}}_r + \dot{\boldsymbol{E}}_{s,r}, \tag{34}$$

for $r = 0,1,\ldots,N$. Detailed derivation of Eqs. (29) and (32) is provided in Lester et al. (2011).

6. Numerical implementation of constitutive laws

Discretizing the relations (19) with an Euler-backward type implicit integrator, we obtain

$$\boldsymbol{\Sigma}_r^{n+1} = \boldsymbol{\Sigma}_r^{n} + \mathcal{L}_r^{n+1} : [\boldsymbol{E}_r^{n+1} - \boldsymbol{E}_r^{n}], \tag{35}$$

where $[\bullet]^n = [\bullet](t_n)$, $t_{n+1} = t_n + \Delta t$ and Δt is a time step.

When considering shrinkage, the above expression needs to account for the shrinkage strains, i.e.

$$\boldsymbol{\Sigma}_r^{n+1} = \boldsymbol{\Sigma}_r^{n} + \mathcal{L}_r^{n+1} : [\boldsymbol{E}_r^{n+1} - \boldsymbol{E}_r^{n} - \boldsymbol{E}_{s,r}^{n+1} + \boldsymbol{E}_{s,r}^{n}]. \tag{36}$$

Eqs. (35) and (36) are nonlinear sets of equations, due to (a) the dependence of the magnetoelastic moduli $\mathcal{L}_r$ on the tensor $\boldsymbol{E}_r$ and (b) the strong nonlinear relation between $\boldsymbol{\varepsilon}_s$ and the magnetic induction $\mathbb{b}$. The second dependence though is only for a very short time period (more like a strain jump), while before and after this period the value of $\mathbb{b}$ remains constant, as Eqs. (11) and (13) indicate. One way to overcome the numerical difficulties of solving such a strongly nonlinear system iteratively, is to "relax" the backward-Euler scheme by considering (a) the magnetomechanical moduli are computed at time t^{n+1} and $\boldsymbol{E}_r^n$

$$\mathcal{L}_r^{n+1} = \mathcal{L}_r^{n+1}(\boldsymbol{E}_r^n, t^{n+1}) \tag{37}$$

and (b) the shrinkage strains at each material constituent are given by

$$\boldsymbol{\varepsilon}_{s,r}^{n+1} = \boldsymbol{\varepsilon}_{s,r}^{n} + [s_r(t^{n+1}, \mathbb{b}_r^n) - s_r(t^n, \mathbb{b}_r^n)]\boldsymbol{I}. \tag{38}$$

With regard to the composite problem when the shrinkage takes place, the macroscopic Eq. (31) can be discretized in a similar manner to (36). Table 1 presents the computational scheme for homogenization which is followed in this work.

7. Numerical examples

7.1. Magnetoelastic particulate composite response during curing, without shrinkage effect

In order to check the validity of the designed framework, a numerical example on a magnetoelastic particulate composite is performed. In the examined composite, cobalt iron oxide ($CoFe_2O_4$) particles are embedded in an epoxy matrix. The particles are assumed to have spherical shape ($a_1 = a_2 = a_3$) and they are randomly distributed inside the matrix.[2]

The material properties of $CoFe_2O_4$ are taken from Huang and Kuo (1997)

[2] Of course the proposed framework allows different type of particle shapes (long or short fibers, general ellipsoids etc). The random distribution of the particles inside the polymer, as Mori–Tanaka considers, is perhaps an inaccurate assumption, since it is well known that, during the curing process, the particles tend to align along the axis of the applied magnetic field. A possible way to overcome such an issue is to assume that the particles due to the magnetic field become ellipsoids with long axis along the direction of the field. For perfectly aligned spherical particles, the periodic homogenization method would be more accurate, but exceeds the scope of this work. The interested reader is referred to Bensoussan et al. (1978), Suquet (1987), Kalamkarov and Kolpakov (1997), Murat and Tartar (1997), Chung et al. (2001), Chung and Kikuchi (2001), Tsalis et al. (2013), Chatzigeorgiou et al. (2015).

Table 1
Computational algorithm for multi-scale approach in curing magneto-elasticity with shrinkage effects.

At time step n everything is known. At time step $n+1$:
1. The magnetomechanical moduli $\mathcal{L}_r$ at each material constituent are computed from Eq. (37)
2. (a) The generalized shrinkage tensor $\boldsymbol{E}_s$ for each material constituent (particles and/or matrix) is evaluated from Eqs. (28) and (38), (b) the effective magnetomechanical tangent modulus $\bar{\mathcal{L}}$ is computed from Eq. (24)
3. The generalized macroscopic shrinkage tensor $\bar{\boldsymbol{E}}_s$ is evaluated from Eq. (29)
4. According to the type of macroscopic loading that is imposed (generalized strain $\bar{\boldsymbol{E}}$ or generalized stress $\bar{\boldsymbol{\Sigma}}$ or mixed conditions), the knowledge of $\bar{\mathcal{L}}$ and $\bar{\boldsymbol{E}}_s$ allows to compute the rest of the macroscopic quantities through Eq. (31)
5. The generalized stress-type tensors $\boldsymbol{\Sigma}$ for the particles and the matrix are computed from Eqs. (32) and (33) respectively
6. The generalized strain-type tensors $\boldsymbol{E}$ for each material constituent is evaluated from Eq. (34)

$$\mathcal{A}_{\mathbb{h}_1} = \begin{bmatrix} 286 & 173 & 170 & 0 & 0 & 0 \\ 173 & 286 & 170 & 0 & 0 & 0 \\ 170 & 170 & 269.5 & 0 & 0 & 0 \\ 0 & 0 & 0 & 45.3 & 0 & 0 \\ 0 & 0 & 0 & 0 & 45.3 & 0 \\ 0 & 0 & 0 & 0 & 0 & 56.5 \end{bmatrix} \cdot 10^9 \text{ Pa},$$

$$\mathcal{C}_{\mathbb{h}_1} = \begin{bmatrix} 0 & 0 & 580.3 \\ 0 & 0 & 580.3 \\ 0 & 0 & 699.7 \\ 0 & 550 & 0 \\ 550 & 0 & 0 \\ 0 & 0 & 0 \end{bmatrix} \text{ N/[Am]},$$

$$\mathcal{K}_{\mathbb{h}_1} = \begin{bmatrix} -590 & 0 & 0 \\ 0 & -590 & 0 \\ 0 & 0 & 157 \end{bmatrix} \cdot 10^{-6} \text{ N/A}^2,$$

while for the epoxy the corresponding tensors are similar to the values given in Pakam and Arockiarajan (2014)

$$\mathcal{A}_{\mathbb{h}_0} = \begin{bmatrix} 5.53 & 2.97 & 2.97 & 0 & 0 & 0 \\ 2.97 & 5.53 & 2.97 & 0 & 0 & 0 \\ 2.97 & 2.97 & 5.53 & 0 & 0 & 0 \\ 0 & 0 & 0 & 1.28 & 0 & 0 \\ 0 & 0 & 0 & 0 & 1.28 & 0 \\ 0 & 0 & 0 & 0 & 0 & 1.28 \end{bmatrix} \cdot 10^9 q(t) \text{ Pa},$$

$$\mathcal{C}_{\mathbb{h}_0} = \mathbf{0}, \quad \mathcal{K}_{\mathbb{h}_0} = \begin{bmatrix} 1.257 & 0 & 0 \\ 0 & 1.257 & 0 \\ 0 & 0 & 1.257 \end{bmatrix} \cdot 10^{-6} \text{ N/A}^2.$$

To account for the curing effect, the matrix tensors $\mathcal{A}_{\mathbb{h}_0}$ has been multiplied by the time dependent, non-dimensional function $q(t)$,

$$q(t) = 0.0001 + [1 - 0.0001][1 - e^{-0.0925t}]$$

where $q_0 = 0.0001$, $q_\infty = 1.0$, $\kappa_q = 0.0925\ \text{s}^{-1}$. Note that here the value of the rate parameter κ_q is $0.0925\ \text{s}^{-1}$ for a 50 s curing time. However, it can be scaled to incorporate any time-span of the curing process by simply changing the value of κ_q. In all the following test cases, two composites with 20% and 60% $CoFe_2O_4$ particles are considered.

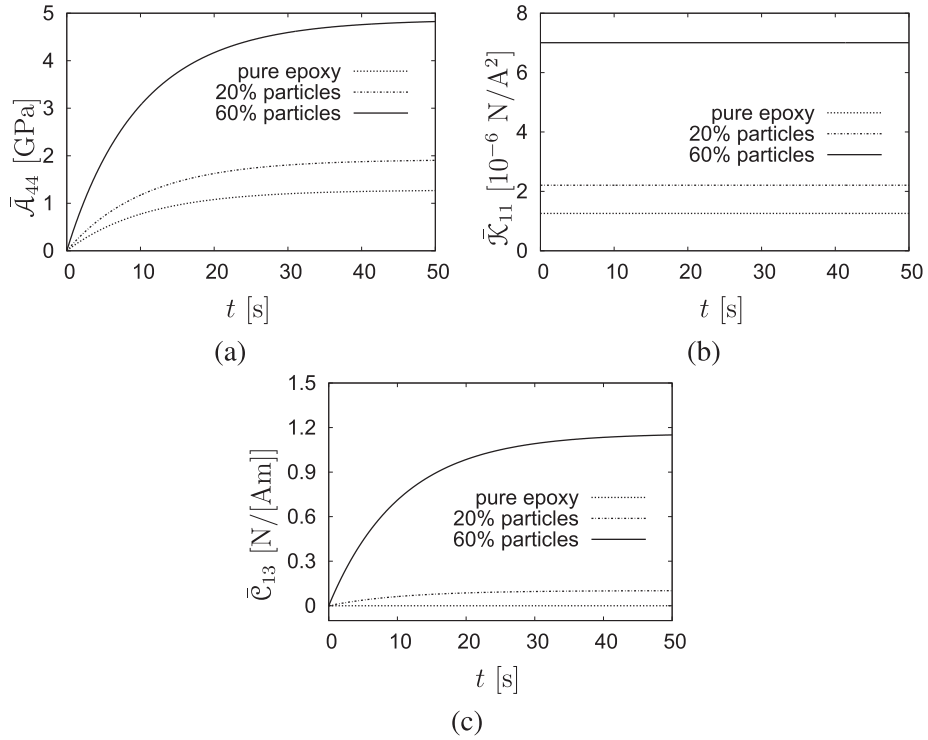

Fig. 2. Evolution with time of macroscopic (a) shear modulus in the 2–3 direction, (b) magnetic permeability in the 1 direction and (c) coupled term $\bar{\mathcal{C}}_{13}$.

We note that such simple constitutive laws for the matrix and the particles, without accounting for the curing term q_t, has been proposed in the literature for magnetomechanical composites (see for instance Huang and Kuo (1997)). More realistic material responses can be proposed by transforming the constitutive laws available in the literature for large deformation magnetomechanical continua to the small deformation framework. Nevertheless, for the scope of the current manuscript the material laws utilized here are sufficient.

7.1.1. Macroscopic magnetomechanical properties

Using these material properties and the micromechanics approach presented in subSection 5.1, the magnetomechanical macroscopic material parameters of the composite can be obtained. Fig. 2 illustrates the evolution with time of three representative macroscopic properties, the shear modulus $\bar{\mathcal{A}}_{44}$, the magnetic permeability $\bar{\mathcal{K}}_{11}$ and the coupled term $\bar{\mathcal{C}}_{13}$. These results are compared with the corresponding ones of the pure epoxy. The macroscopic shear modulus of the composite follows a similar trend as the shear modulus of the epoxy, since it evolves exponentially with time (Fig. 2a). The magnetic permeability increases more than five times with the presence of 60% particles, but still remains independent of time (Fig. 2b). The most interesting observation appears with the coupled terms: while the pure epoxy is considered to have no piezomagnetic response, the composite coupled terms not only exist, but they also evolve with time in an exponential way, as Fig. 2c shows. Similar conclusions are obtained for the rest of the composite magnetomechanical coefficients.

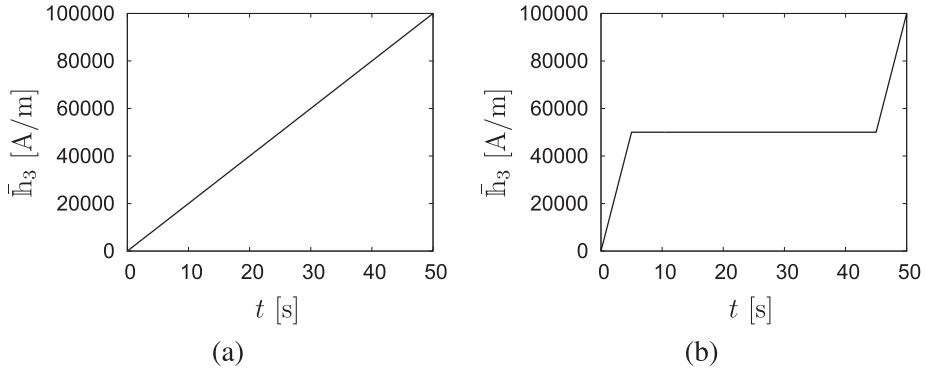

Fig. 3. (a) Linear and (b) stepwise evolution with time of macroscopic magnetic fieldin the 3 direction.

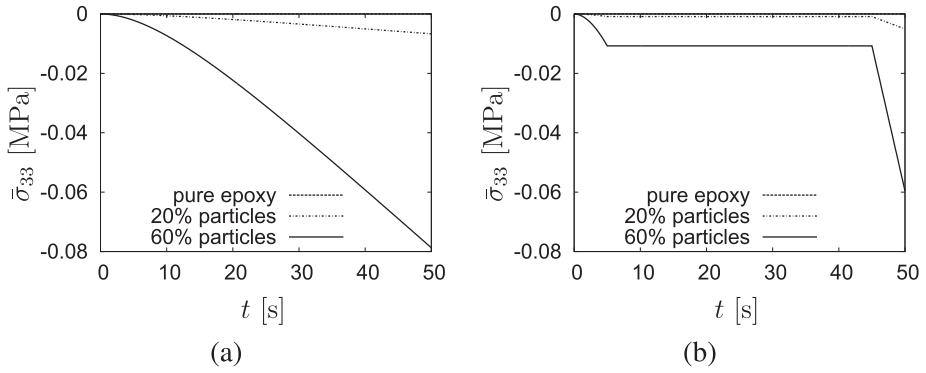

Fig. 4. Evolution with time of macroscopic stress in the 3 direction when the evolution of the macroscopic field is (a) linear and (b) stepwise. No macroscopic strain is applied.

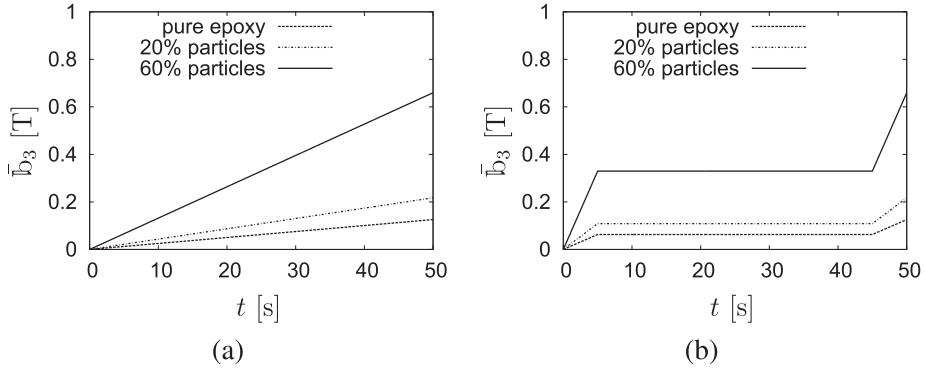

Fig. 5. Evolution with time of macroscopic magnetic induction in the 3 direction when the evolution of the macroscopic field is (a) linear and (b) stepwise. No macroscopic strain is applied.

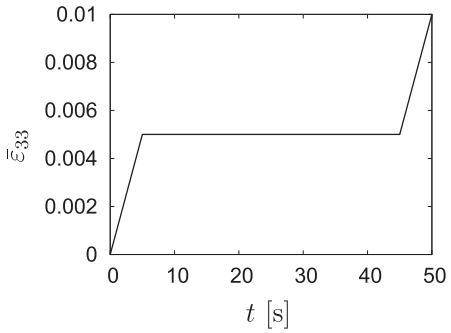

Fig. 6. Stepwise evolution with time of macroscopic strain in the 3 direction.

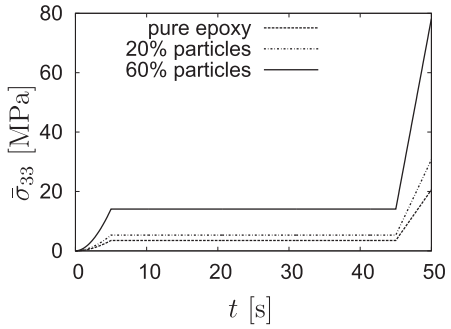

Fig. 7. Evolution with time of the macroscopic stress in the 3 direction when a stepwise strain with time is considered. No macroscopic magnetic field.

7.1.2. Case 1: no applied strain

Here it is considered that there is zero macroscopic strain in the 3 direction (plane strain macroscopic conditions), the directions 1 and 2 are traction free, and two different cases of macroscopic magnetic field are examined: (a) linearly increasing (Fig. 3a) with time in the 3 direction until it reaches the value of 100,000 A/m, (b) stepwise increasing (Fig. 3b) with time in the 3 direction: two linear increases with time for 5 s, separated by a period of 40 s in which the magnetic field is constant. The maximum magnetic field reaches the value of 100,000 A/m. As it is illustrated in Fig. 4, the macroscopically applied magnetic field influences the stress in the 3 direction only when $CoFe_2O_4$ particles are present, causing compressive conditions inside the composite. Note that the stress, though very small in magnitude, in the third load step (45–50 s) is higher than the first step (0–5 s) since there is a minor evolution of the coupled parameters, cf. Fig. 2c. The macroscopic magnetic induction on the other hand shows a similar trend with the applied

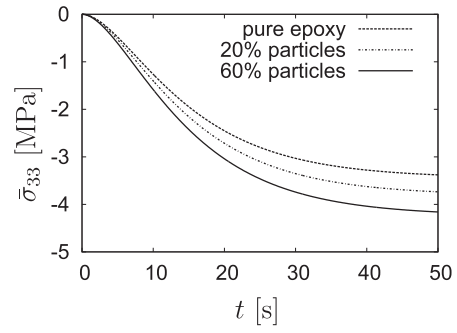

Fig. 9. Evolution with time of macroscopic normal stress in the 3 direction under a zero macroscopic strain and magnetic field. Shrinkage effects are taken into account.

magnetic field (Fig. 5). For the case of step-wise magnetic load, the increase of the stress in the last load phase is higher than the increment in the first phase. This is due to an evolution, though very small in magnitude, of the coupled parameters.

7.1.3. Case 2: stepwise applied strain

Here it is considered that there is an applied macroscopic strain in the 3 direction which follows three steps with time: a linear increase for 5 s, a constant value for 40 s and again a linear increase for 5 s, until it reaches the value 0.01 (Fig. 6). The directions 1 and 2 are considered traction free. For the macroscopic magnetic field three cases are examined: (a) no field, (b) linear increasing and (c) stepwise.

7.1.3.1. No macroscopic magnetic field. If we do not apply any magnetic field, the magnetic induction of the composite is almost zero, due to the small value of the coupled terms. The evolution of the macroscopic stress appears in Fig. 7 and follows a stepwise relation with time similar to the one of the strain. For 60% particles, it is observed a sharp increase in stress between 0–5 s and 45–50 s, and moreover the final value of stress ($\bar{\sigma}_{33}$) is almost four times larger than that of the pure epoxy. Due to the successive chain cross-linking during the holding phase (5–45 s), the stress increment in the third phase is much higher than in the first phase (0–5 s).

7.1.3.2. Linear and stepwise evolution of macroscopic magnetic field with time. When the evolutions of magnetic field of Fig. 3 are considered, the stress evolution with time does not present noticeable difference from that displayed in Fig. 7, and the macroscopic magnetic induction shows to follow the same trend as the macroscopic

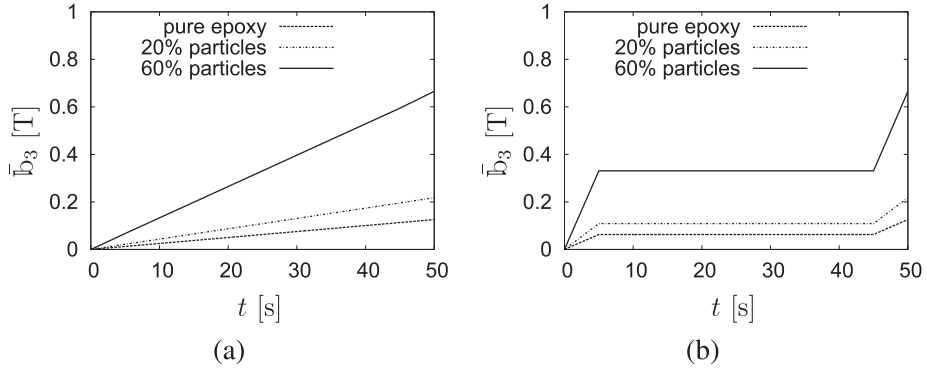

Fig. 8. Evolution with time of macroscopic magnetic induction in the 3 direction when a stepwise strain with time is considered and the evolution of the macroscopic field is (a) linear and (b) stepwise.

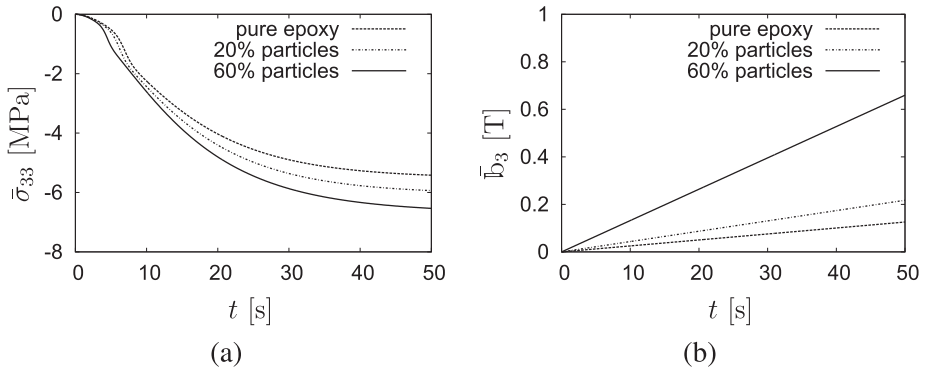

Fig. 10. Evolution with time of (a) macroscopic normal stress in the 3 direction and (b) macroscopic magnetic induction in the 3 direction, when the macroscopic magnetic field increases linearly and the macroscopic strain is zero. Shrinkage effects are taken into account.

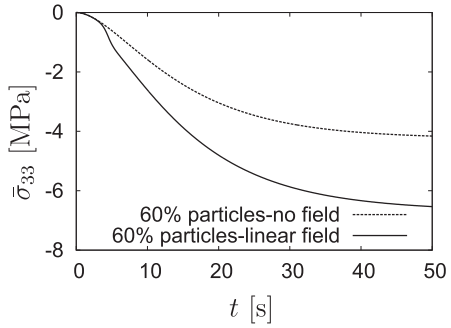

Fig. 11. Effect of the magnetic field on the evolution of the macroscopic normal stress with time. Shrinkage effects are taken into account.

magnetic field, independently of the strain path (Fig. 8). This is due to the small macroscopic coupled coefficients, which cause the mechanical and the magnetic phenomena to appear almost decoupled when a considerable strain and a magnetic field are applied.

7.2. Magnetoelastic particulate composite response during curing, with shrinkage effect

In the next examples, the influence of the shrinkage effect will be studied. The epoxy is assumed to have a total shrinkage of the form

$$s(t) = s_\infty[1 - \exp(-0.0925t)],$$
$$s_\infty = 0.0025 + 0.0005\tanh(5[e - 0.055]).$$

We examine two cases: *(a) zero macroscopic strain and magnetic field and (b) zero macroscopic strain and linearly increasing magnetic field.*

(a) Zero macroscopic strain and magnetic field

It is considered that a zero macroscopic strain is enforced in the 3 direction, while the directions 1 and 2 are traction free. Moreover, a zero macroscopic magnetic field is applied. The evolution of macroscopic stress with the curing time is illustrated in Fig. 9. As is illustrated in Fig. 9, without the application of any external load (mechanical or magnetic), there is a significant stress generation due to the curing process. Moreover, as it is observed with the application of an external load (mechanical or magnetic), at approximately 5 s, the effect of shrinkage causes a change in the slope of the curves for both the pure epoxy and the composite.

(b) Zero macroscopic strain and linearly increasing magnetic field

Here the difference with the previous case is that the macroscopic magnetic field increases linearly with time, following the path of Fig. 3a. The corresponding results are illustrated in Fig. 10. We observe that the stress has been increased substantially due to the presence of the magnetic field by almost 50% with regard to the previous case (Fig. 11). It is due to the fact that the presence of a magnetic load during the curing makes the material stiffer and handicaps a sample to shrink. However, the shrinkage does not effect the magnetic induction (i.e. compared with Fig. 8a). This example is analogous with the first case of 7.1.2 (zero strain, linearly increasing magnetic field). As it is observed from Figs. 4a and 10a, the shrinkage effects provide a tremendous increase in the stress levels of the composite at the end of the curing process (6 MPa compared to 0.08 MPa for 60% particles volume fraction).

8. Conclusion and outlook

In this paper, we propose a multi-scale approach for the simulation of polymeric materials during curing processes in the case of a magneto-mechanical coupled load. Starting from the idea of continuous chain crosslinking, a convolution integral type potential function is proposed which is then evaluated with the help of the second law of thermodynamics to develop a hypoelastic type constitutive relation for a magneto-mechanical coupled process in the small strain setting. The curing-induced shrinkage phenomenon is a major pathological event in the process. A novel coupled framework is also proposed to capture the shrinkage behavior where the total amount of shrinkage is not only dependent on the curing time but also on the duration and the magnitude of the application of magnetic loads. Based on a set of reasonable material parameters from the literature, several relevant examples are presented by using a Mori–Tanaka type semi-analytical homogenization method which is extended by Dunn and Taya (1993) for the case of magneto-mechanical composite materials. All numerical examples show that the proposed models can capture major phenomena observable in the curing process under a magneto-mechanically coupled load. In a forthcoming contribution, we will extend the idea to a computational homogenization realm so that real boundary value problems can be simulated. There are also plans to extend the ideas to a finite strain setting since mostly polymeric materials can undergo large deformations. The curing phenomenon is an exothermic reaction process. Therefore, the proposed model needs to be extended to take into account for temperature evolution during the process. In this case, a magneto-thermo-mechanical problem has to be considered.

Acknowledgment

This work is funded by an ERC advanced grant within the project MOCOPOLY.

References

Aboudi, J., Pindera, M.-J., Arnold, S.M., 2003. Higher-order theory for periodic multiphase materials with inelastic phases. Int. J. Plast. 19 (6), 805–847.

Asada, T., Ohno, N., 2007. Fully implicit formulation of elastoplastic homogenization problem for two-scale analysis. Int. J. Solids Struct. 44 (22–23), 7261–7275.

Bensoussan, A., Lions, J., Papanicolaou, G., 1978. Asymptotic methods for periodic structures. North Holland.

Bensoussan, A., Lions, J., Papanicolaou, G., 1978. Asymptotic Methods for Periodic Structures. North Holland.

Boczkowska, A., Awietjan, S.F., 2009. Smart composites of urethane elastomers with carbonyl iron. J. Mater. Sci. 44, 4104–4111.

Borcea, L., Bruno, O., 2001. On the magneto-elastic properties of elastomer-ferromagnet composites. J. Mech. Phys. Solids 49, 2877–2919.

Böse, H., Rabindranath, R., Ehrlich, J., 2012. Soft magnetorheological elastomers as new actuators for valves. J. Intell. Mater. Syst. Struct. 23, 989–994.

c, K., Kikuchi, N., 2001. A class of general algorithms for multi-scale analyses of heterogeneous media. Comput. Methods Appl. Mech. Eng. 190, 542764.

Charalambakis, N., 2010. Homogenization techniques and micromechanics. A survey and perspectives. Appl. Mech. Rev. 63 (3), 030803.

Chatzigeorgiou, G., Javili, A., Steinmann, P., 2014. Unified magnetomechanical homogenization framework with application to magnetorheological elastomers. Math. Mech. Solids 19 (2), 194–212.

Chatzigeorgiou, G., Chemisky, Y., Meraghni, F., 2015. Computational micro to macro transitions for shape memory alloy composites using periodic homogenization. Smart Mater. Struct. 24, 035009.

Chen, L., Gong, X.L., Jiang, W.Q., Yao, J.J., Deng, H.X., Li, W.H., 2007. Investigation on magnetorheological elastomers based on natural rubbers. J. Mater. Sci. 42, 5483–5499.

Chung, P.W., Tamma, K.K., Namburu, R.R., 2001. Asymptotic expansion homogenization for heterogeneous media: computational issues and applications. Compos.: Part A 32, 12911301.

Danas, K., Kankanala, S.A., Triantafyllidis, 2012. Experiments and modelling of iron-particle-filled. J. Mech. Phys. Solids 60 (1), 120–138.

Dunn, M.L., Taya, M., 1993. Micromechanics predictions of the effective electroelastic moduli of piezoelectric composites. Int. J. Solids Struct. 30 (2), 161–175.

Feyel, F., Chaboche, J.-L., 2000. FE2 multiscale approach for modelling the elastoviscoplastic behaviour of long fibre SiC/Ti composite materials. Comput. Methods Appl. Mech. Eng. 183 (3–4), 309–330.

Galipeau, E., Ponte Castañeda, P., 2013. A finite-strain constitutive model for magnetorheological elastomers: magnetic torques and fiber rotations. J. Mech. Phys. Solids 61 (4), 1065–1090.

Gavazzi, A.C., Lagoudas, D.C., 1990. On the numerical evaluation of Eshelby's tensor and its application to elastoplastic fibrous composites. Comput. Mech. 7, 13–19.

Geers, M.G.D., Kouznetsova, V.G., Brekelmans, W.A.M., 2010. Multi-scale computational homogenization: trends and challenges. J. Comput. Appl. Math. 234 (7), 2175–2182.

Gillen, K.T., 1988. Effect of cross-links which occur during continuous chemical stress-relaxation. Macromolecules 21, 442–446.

Guedes, J., Kikuchi, N., 1990. Preprocessing and postprocessing for materials based on the homogenization method with adaptive finite element methods. Comput. Methods Appl. Mech. Eng. 83 (2), 142–198.

Hashin, Z., Shtrikman, S., 1963. A variational approach to the theory of the elastic behaviour of multiphase materials. J. Mech. Phys. Solids 11 (2), 127–140.

Heinrich, C., Aldridge, M., Wineman, A.S., Kieffer, J., Waas, A.M., Shahwan, K.W., 2013. The role of curing stresses in subsequent response, damage and failure of textile polymer composites. J. Mech. Phys. Solids 61, 1241–1264.

Hill, R., 1963. Elastic properties of reinforced solids: some theoretical principles. J. Mech. Phys. Solids 11, 357–372.

Hill, R., Rice, J., 1972. Constitutive analysis of elastic–plastic crystals at arbitrary strain. J. Mech. Phys. Solids 20 (6), 401–413.

Hojjati, M., Johnston, A., Hoa, S.V., Denault, J., 2004. Viscoelastic behaviour of Cytec FM73 adhesive during cure. J. Appl. Polym. Sci. 91, 2548–2557.

Hossain, M., Steinmann, P., 2014. Degree of cure-dependent modelling for polymer curing processes at small-strain. Part I: consistent reformulation. Comput. Mech. 53 (4), 777–787.

Hossain, M., Possart, G., Steinmann, P., 2009a. A small-strain model to simulate the curing of thermosets. Comput. Mech. 43, 769–779.

Hossain, M., Possart, G., Steinmann, P., 2009b. A finite strain framework for the simulation of polymer curing. Part I: elasticity. Comput. Mech. 44 (5), 621–630.

Hossain, M., Saxena, P., Steinmann, P., 2015a. Modelling the mechanical aspects of the curing process in magneto-sensitive elastomeric materials. Int. J. Solids Struct. 58, 257–269.

Hossain, M., Saxena, P., Steinmann, P., 2015b. Modelling the curing process in magneto-sensitive polymers: rate-dependence and shrinkage. Int. J. Non-Linear Mech. http://dx.doi.org/10.1016/j.ijnonlinmec.2015.04.008.

Huang, J.H., Kuo, W.-S., 1997. The analysis of piezoelectric/piezomagnetic composite materials containing ellipsoidal inclusions. J. Appl. Phys. 81 (3), 1378–1386.

Javili, A., Chatzigeorgiou, G., Steinmann, P., 2014. Computational homogenization in magneto-mechanics. Int. J. Solids Struct. 50 (25), 4197–4216.

Johlitz, M., 2012. On the representation of ageing phenomena. J. Adhes. 88 (7), 620–648.

Johlitz, M., Lion, A., 2013. Chemo-thermomechanical ageing of elastomers based on multiphase continuum mechanics. Cont. Mech. Therm. 25 (5), 605–624.

Jolly, M.R., Carlson, J.D., Muñoz, B.C., 1996. A model of the behaviour of magnetorheological materials. Smart Mater. Struct. 5, 607–614.

Kalamkarov, A.L., Kolpakov, A.G., 1997. Analysis, Design and Optimization of Composite Structures. Wiley.

Kaleta, J., Krolewicz, M., Lewandowski, D., 2011. Magnetomechanical properties of anisotropic and isotropic magnetorheological composites with thermoplastic elastomer matrices. Smart Mater. Struct. 20, 1–12.

Kanouté, P., Boso, D.P., Chaboche, J.L., Schrefler, B.A., 2009. Multiscale methods for composites: a review. Arch. Comput. Meth. Eng. 16, 31–75.

Kiasat, M., 2000. Curing shrinkage and residual stresses in viscoelastic thermosetting resins and composites (PhD thesis). TU Delft, The Netherlands.

Klinge, S., Bartels, A., Steinmann, P., 2012. Modeling of curing processes based on a multi-field potential: single and multi-scale aspects. Int. J. Solids Struct. 49, 2320–2333.

Klinge, S., Bartels, A., Steinmann, P., 2012. The multi-scale approach to the curing of polymer incorporating viscous and shrinkage effects. Int. J. Solids Struct. 49, 3883–3990.

Kouznetsova, V., Brekelmans, W.A.M., Baaijens, F.P.T., 2001. An approach to micro-macro modeling of heterogeneous materials. Comput. Mech. 27 (1), 37–48.

Lagoudas, D.C., Gavazzi, A.C., Nigam, H., 1991. Elastoplastic behavior of metal matrix composites based on incremental plasticity and the Mori–Tanaka averaging scheme. Comput. Mech. 8, 193–203.

Lester, B.T., Chemisky, Y., Lagoudas, D.C., 2011. Transformation characteristics of shape memory alloy composites. Smart Mater. Struct. 20 (9), 094002.

Levin, V.M., Michelitsch, T., Sevostianov, I., 2000. Spheroidal inhomogeneity in a transversely isotropic piezoelectric medium. Arch. Appl. Mech. 70, 673–693.

Liebl, C., Johlitz, M., Yagimli, B., Lion, A., 2012. Three-dimensional chemo-thermomechnically coupled simulation of curing adhesives including viscoplasticity and chemical shrinkage. Comput. Mech. 49 (5), 603–615.

Lion, A., Höfer, P., 2007. On the phenomenological representation of curing phenomena in continuum mechanics. Arch. Mech. 59, 59–89.

Mahnken, R., 2013. Thermodynamic consistent modeling of polymer curing coupled to viscoelasticity at large strains. Int. J. Solids Struct. 50, 2003–2021.

Michel, J.C., Moulinec, H., Suquet, P., 1999. Effective properties of composite materials with periodic microstructure: a computational approach. Comput. Methods Appl. Mech. Eng. 172 (1–4), 109–143.

Miehe, C., 2002. Strain-driven homogenization of inelastic microstructures and composites based on an incremental variational formulation. Int. J. Numer. Meth. Eng. 55 (11), 1285–1322.

Miehe, C., Koch, A., 2002. Computational micro-to-macro transitions of discretized microstructures undergoing small strains. Arch. Appl. Mech. 72 (4–5), 300–317.

Mura, T., 1987. Micromechanics of Defects in Solids. Martinus Nijhoff Publishers.

Murat, F., Tartar, L., 1995. H-convergence. In: Kohn R.V., (Ed.), Topics in the Mathematical Modeling of Composite Materials, Progress in Non-linear Differential Equations and their Applications.

Murat, F., Tartar, L., 1997. H-convergence. In: Cherkaev, A., Kohn, R. (Eds.), Topics in the Mathematical Modelling of Composite Materials (Progress in Nonlinear Differential Equations and their Applications vol. 31) 2143. Birkhäuser.

Pakam, N., Arockiarajan, A., 2014. Study on effective properties of 1-3-2 type magneto-electro-elastic composites. Sens. Actuators A: Phys. A209, 87–99.

Pindera, M.-J., Khatam, H., Drago, A.S., Bansal, Y., 2009. Micromechanics of spatially uniform heterogeneous media: a critical review and emerging approaches. Compos. Part B: Eng. 40 (5), 349–378.

Ponte Castañeda, P., 1996. Exact second-order estimates for the effective mechanical properties of nonlinear composite materials. J. Mech. Phys. Solids 44 (6), 827–862.

Ponte Castañeda, P., Galipeau, E., 2011. Homogenization-based constitutive models for magneto-rheological elastomers at finite strain. J. Mech. Phys. Solids 59 (2), 194–215.

Qu, J., Cherkaoui, M., 2006. Fundamentals of Micromechanics of Solids. Wiley.

Schröder, J., Keip, M.A., 2012. Two-scale homogenization of electromechanically coupled boundary value problems. Comput. Mech. 50 (2), 229–244.

Smit, R.J.M., Brekelmans, W.A.M., Meijer, H.E.H., 1998. Prediction of the mechanical behavior of nonlinear heterogeneous systems by multi-level finite element modeling. Comput. Methods Appl. Mech. Eng. 155 (1–2), 181–192.

Suquet, P.M., 1987. Elements of homogenization for inelastic solid mechanics. Lect. Notes Phys. 272, 193–278.

Suquet, P.M., 1987. Elements of homogenization for inelastic solid mechanics. Lect. Notes Phys. 272, 193278.

Terada, K., Kikuchi, N., 1995. Nonlinear homogenization method for practical applications. In: Ghosh, S., Ostoja Starzewski, M. (Eds.), Computational Methods in Micromechanics, vol. AMD-212/MD-62. ASME, pp. 1–16.

Terada, K., Kikuchi, N., 2001. A class of general algorithms for multi-scale analyses of heterogeneous media. Comput. Methods Appl. Mech. Eng. 190, 5427–5464.

Tsalis, D., Baxevanis, T., Chatzigeorgiou, G., Charalambakis, N., 2013. Homogenization of elastoplastic composites with generalized periodicity in the microstructure. Int. J. Plast. 51, 16187.

Varga, Z., Filipcsei, G., Zrínyi, M., 2006. Magnetic field sensitive functional elastomers with tuneable elastic modulus. Polymer 47, 227–233.

Wang, D., Chen, J.-S., Sun, L., 2003. Homogenization of magnetostrictive particle-filled elastomers using an interface-enriched reproducing kernel particle method. Finite Elem. Anal. Des. 39 (8), 765–782.
Xu, Y., Gong, X., Xuan, S., Zhang, W., Fan, Y., 2011. A high-performance magnetorheological material: preparation, characterization and magnetic–mechanic coupling properties. Soft Matter 7 (11), 5246–5254.
Yin, H.M., Sun, L.Z., Chen, J.S., 2002. Micromechanics-based hyperelastic constitutive modeling of magnetostrictive particle-filled elastomers. Mech. Mater. 34, 505–516.
Yin, H.M., Sun, L.Z., Chen, J.S., 2006. Magneto-elastic modeling of composites containing chain-structured magnetostrictive particles. J. Mech. Phys. Solids 54, 975–1003.
Yvonnet, J., Gonzalez, D., He, Q.-C., 2009. Numerically explicit potentials for the homogenization of nonlinear elastic heterogeneous materials. Comput. Methods Appl. Mech. Eng. 198 (33–36), 2723–2737.
Zhou, G., 2003. Shear properties of a magnetorheological elastomer. Smart Mater. Struct. 12, 139–146.